ISSN 1392–124X (print), ISSN 2335–884X (online) INFORMATION TECHNOLOGY AND CONTROL, 2016, T. 45, Nr. 1

Path Following for Unmanned Helicopter: An Approach on Energy Autonomy Improvement

Daniel C. Gandolfo, Lucio R. Salinas, Juan M. Toibero

Instituto de Automática (INAUT), National University of San Juan (UNSJ),
National Scientific and Technical Research Council (CONICET), San Juan, Argentina
e-mail: dgandolfo@inaut.unsj.edu.ar, lsalinas@inaut.unsj.edu.ar, mtoibero@inaut.unsj.edu.ar

Alexandre Brandão

Núcleo de Especialização em Robótica (NERO),
Department of Electrical Engineering, Federal University of Viçosa, Viçosa, MG Brazil
e-mail: alexandre.brandao@ufv.br

crossref http://dx.doi.org/10.5755/j01.itc.45.1.12413

Abstract. In the last decades, research efforts related to Unmanned Aerial Vehicles (UAV) have grown substantially in terms of control stabilization and navigation strategies. However, the energy available on board is finite and this is a limiting factor that prevents engineers from coming up with the best aerial solution in many situations. In this paper the path following control of a helicopter UAV based on the kinematic model is proposed using a feedback linearization technique. The helicopter speed is adjusted according to direction changes of the desired path. Thus, the aircraft should holds its own weight in the air for the shortest possible time, aiming to save energy without neglecting the position control errors which can accumulate when its velocity increases and path direction changes. The proposed controller output is coupled to a dynamic model of a helicopter in order to evaluate the dynamic effects and to adjust the controller parameters. The stability of the controller is demonstrated in the sense of Lyapunov theory and validated by simulation results.

Keywords: Unmanned Aerial Vehicles; Path Following Controller; Position Control Errors; Traveled Path.

1. Introduction

In the last two decades, the projection of different UAVs (unmanned aerial vehicles) from the military to the civilian sector has promoted the increase of such applications in aerial robots. The research efforts related to this kind of mobile robots are gaining support in several applications because there are many situations where it is very useful to have a high point of view (in terms of altitude) or to place a sensor in an inaccessible area. Nowadays it is possible to find several models of UAV capable to take off, develop a scheduled flight and land autonomously. There are many important applications for UAVs, however, the limited energy on board is a great threat that often makes the mission assigned to the UAV harder or impossible to complete. Currently, the electrical energy storage sources have evolved considerably (such as lithium polymer batteries), yet devices used as propulsion systems (such as electrical motors) still require a great amount of energy during flight. Thus the autonomy is a big challenge in terms of navigation control of UAVs and some research efforts need to be focused in such area in order to increase the viability of the missions designed for UAVs. This problem is enhanced in rotary wings vehicles (helicopters and multi-copters) where energy consumption is high compared to other aircraft (airplanes and blimps) [1].

Multidisciplinary approaches have been reported on the bibliography to increase the total flight time from different UAVs (aerodynamics, structural, materials technology, energy harvesting, path planning, among others). However many of them are related to the UAV constructive aspects, the environment in which it is moving, the mission assigned to it and the possibility to harvest energy from the environment. In other words they are particular cases of the saving energy problem. For example, it is not possible to add solar films on a helicopter (because it has no fixed wing surface) nor to have ceiling attachment in a fixed wing UAV while

offering a panoramic view of the environment as done in [2] for a quadrotor. Nevertheless, there is always a common point to all the particularities: the control law used to command the UAV during a desired mission. Therefore, the control law is a flexible and broad field which can be studied as an alternative to increase the total flight time of UAVs. In this context the present work is framed and focused on rotary wing aircraft. In the literature one can find numerous reports on the control of rotary wing aircraft in which different control laws are presented, as nonlinear controller based on the theory of Lyapunov [3], neural networks controller [4], controller based on fuzzy logic [5], predictive controller [6] and controller based on linear algebra theory [7]. In most cases the primary objective is to track a desired reference with bounded position errors through a stable control law, and the energy consumption or total flight time are not taken into account. In some works the authors aim to minimize control actions, such as in [8], where a linear quadratic controller is used for trajectory tracking of a Tri-TiltRotor. Thus the control law is achieved by minimizing a performance index that considers control actions and position errors in a weighted way.

For trajectory tracking, a space-time restriction must be respected during the aircraft following mission (ie, the aircraft must reach a given point at a given time). Therefore, there exist a specific value of control action which must be delivered by any control law, regardless of the technique complexity (the control strategy can conveniently modify transient response, which is the way the control action is achieved). Such inflexibility suggests that the trajectory tracking technique does not allow significant energy savings. On the other hand, in the path-following approach, the speed at which the path is traversed remains an extra degree of freedom [9]; this can be used to accomplish other goals, in this case, complete the mission with less energy consumption. This is a very important thing to keep in mind and motivates the study of path following techniques.

There are numerous reports in the literature of controllers for different types of UAVs based on different control techniques. In [10] a nonlinear controller allows the UAV to follow a predefined path. The controller parameters are adjusted by a fuzzy logic rule. A new method for UAV to follow the 2-D defined path is presented in [11] which consists of the out guidance loop and the inner control loop. The guidance law relies on the idea of tracking the virtual target that travels along the path. The speed of the virtual target is explicitly specified and related to the motion of the real aircraft by a fictitious mechanical link. The control strategy proposed by the authors in [12] is based on the idea that the UAV model is constituted of two subsystems. Then the attitude control is proposed using an integral sliding mode control, and a simple PID is used for the positioning control (motion in the x-y plane). Based on accuracy, robustness and control efforts, the authors in [13] compare the performance of different path following algorithms for UAVs considering only the kinematic model.

Commonly in the literature, the primary objective is to keep the path tracking error bounded (or tending to zero) and the traversed speed fixed [14] or adjusted only for achieving the target. In some cases, this primary objective is still sought in the presence of faults in the aircraft actuators and the control technique is focused on getting enough robustness, as is proposed by the authors in [15]. Furthermore, in most cases the results are based on the kinematic model of the aircraft with no consideration of its dynamic components [16],[17].

In the present work, a control strategy to guide a rotorcraft UAV is proposed based on its kinematic model. A feedback linearization technique is applied here considering the vehicle speed as a free variable (it is not left constant during the mission execution), which changes its value according to the geometric requirements of the desired path and the aircraft's maximum speed. Because helicopters have not fixed-wing surface its own weight must be maintained by the main rotor all the time, hence, they should execute the mission in the shortest possible time aiming to save energy without neglecting the position control errors which can accumulate when its velocity increases and path direction changes. The proposed controller output is coupled to a dynamic model of a helicopter (presented in [18]) in order to evaluate the dynamic effects and to adjust the controller parameters. The stability of the controller is demonstrated in the sense of Lyapunov theory and validated by simulation results.

2. UAV Kinematic Model

The complete kinematic model of UAV is complex when trying to analyze mathematically, then simplified models are often used to design the controllers.

Consider a rotorcraft UAV positioned at any distance with respect to an inertial coordinate system called $\langle g \rangle$, where the x axis point to east, the y axis points to north and the z axis points up (ENU system). Then, making a simplification respect to the complete model, it is possible to consider that the UAV cannot perform pitching and rolling movements (roll = pitch = 0); that is, it cannot rotate about two of its three axes. Then, this new model has only four degrees of freedom. The vehicle motion is governed by the combined action of four variables: three linear velocities v_{ax}, v_{ay}, v_{az} and one angular velocity ω_{az}, defined in the Cartesian rotational system called $\langle s \rangle$ in the body of the aircraft. As the pitch and roll angles are restricted, then $\omega_{ax} = \omega_{ay} = 0$. Each linear velocity of the UAV always points to one axis related to system

$\langle s \rangle$; v_{az} always points up in the same direction as the z axis; v_{ax} and v_{ay} point forward and to the left of the vehicle respectively. The angular velocity ω_{az} rotates the system $\langle s \rangle$ around its z axis (viewed from above). Then, the set of simplified kinematic equations that relate the position (x_a, y_a, z_a) and the orientation ψ_a of the UAV is

$$\begin{cases} \dot{x}_a = v_{ax}\cos\psi_a - v_{ay}\sin\psi_a \\ \dot{y}_a = v_{ax}\sin\psi_a + v_{ay}\cos\psi_a \\ \dot{z}_a = v_{az} \\ \dot{\psi}_a = \omega_{az} \end{cases} \quad (1)$$

where (x_a, y_a, z_a) and ψ_a are calculated with respect to the inertial frame $\langle g \rangle$.

3. Path Following Control

The objective of the path following problem is to control the helicopter to follow a predefined path in R^3 while attaining a 3-D desired velocity and yaw angle. Then, given a geometric path $P \in \mathsf{R}^3$, the strategy should find continuous control actions such that, under appropriate initial conditions, the following goals are reached: a) The rotorcraft asymptotically converges to P; b) The velocity $V_a = \sqrt{v_{ax}^2 + v_{ay}^2 + v_{az}^2}$ asymptotically converges to a desired value V_d, and c) The yaw angle ψ_a asymptotically converges to a desired value ψ_r dependent on the helicopter displacement along P. Fig. 1 illustrates this statement.

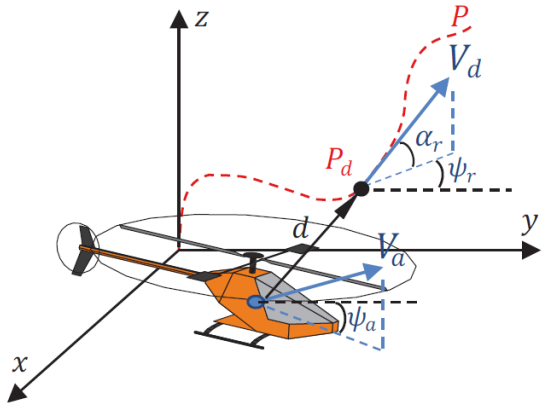

Figure 1. Graphical representation of the helicopter and the desired path

In Fig. 1, d represents the shortest distance between the aircraft and the path, which is a function of the aircraft position (x_a, y_a, z_a) and P_d position given by (x_r, y_r, z_r).

3.1. Path following control law

Next, the kinematic path following controller is presented, which is based on feedback linearization. The set of equations (1) can be expressed in matrix form as follows

$$\begin{bmatrix} \dot{x}_a \\ \dot{y}_a \\ \dot{z}_a \\ \dot{\psi}_a \end{bmatrix} = \begin{bmatrix} c_{\psi_a} & -s_{\psi_a} & 0 & 0 \\ s_{\psi_a} & c_{\psi_a} & 0 & 0 \\ 0 & 0 & 1 & 0 \\ 0 & 0 & 0 & 1 \end{bmatrix} \begin{bmatrix} v_{ax} \\ v_{ay} \\ v_{az} \\ \omega_{az} \end{bmatrix} \Rightarrow \dot{\mathbf{x}} = \mathbf{J}\mathbf{v}_\mathbf{a}, \quad (2)$$

where $\dot{\mathbf{x}} = [\dot{x}_a \quad \dot{y}_a \quad \dot{z}_a \quad \dot{\psi}_a]^{\mathrm{T}}$ is the position vector of the aircraft in the inertial reference frame $\langle g \rangle$, $\mathbf{v_a} = [v_{ax} \quad v_{ay} \quad v_{az} \quad \omega_{az}]^{\mathrm{T}}$ is the speed vector in the frame reference $\langle s \rangle$ and $\mathbf{J}$ represents the Jacobean matrix that relates them (we use c_{ψ_a} for $\cos\psi_a$ and s_{ψ_a} for $\sin\psi_a$).

The following control law $\mathbf{v_a}$ is proposed to the kinematic controller

$$\mathbf{v_a} = \mathbf{J}^{-1}\mathbf{y}, \quad (3)$$

being $\mathbf{J}^{-1}$ the inverse of $\mathbf{J}$ (2) and

$$\mathbf{y} = \mathbf{K_s}\tanh(\mathbf{K}\tilde{\mathbf{x}}) + \mathbf{v_d} \quad (4)$$

In (4), $\tanh$ is the hyperbolic tangent function operating element-wise; $\mathbf{K_s}$ and $\mathbf{K}$ are two positive constant diagonal matrices, selected to give a maximum value to the control actions and to modify the hyperbolic tangent mapping of the position error vector respectively

$$\mathbf{K_s} = \begin{bmatrix} k_{sx} & 0 & 0 & 0 \\ 0 & k_{sy} & 0 & 0 \\ 0 & 0 & k_{sz} & 0 \\ 0 & 0 & 0 & k_{s\psi} \end{bmatrix}, \mathbf{K} = \begin{bmatrix} k_x & 0 & 0 & 0 \\ 0 & k_y & 0 & 0 \\ 0 & 0 & k_z & 0 \\ 0 & 0 & 0 & k_\psi \end{bmatrix}.$$

$\mathbf{v_d}$ is the desired velocity vector

$$\mathbf{v_d} = \begin{bmatrix} v_{dx} \\ v_{dy} \\ v_{dz} \\ \omega_{dz} \end{bmatrix} = \begin{bmatrix} V_d\cos(\alpha_r)\cos(\psi_r) \\ V_d\cos(\alpha_r)\sin(\psi_r) \\ V_d\sin(\alpha_r) \\ 0 \end{bmatrix} \quad (5)$$

with

$$\psi_r = atan2\left(\frac{\Delta_{y_r}}{\Delta_{x_r}}\right), \quad \alpha_r = \arctan\left(\frac{\Delta_{z_r}}{\sqrt{\Delta_{x_r}^2 + \Delta_{y_r}^2}}\right);$$

where $atan2$ is the four quadrant arctangent function, ψ_r represents the direction of the path tangent vector at $\mathbf{x_r}$ (point of minimum distance between the path and the aircraft) projected on the XY-plane, and α_r

represents the elevation angle measured from the XY-plane to the path tangent vector at $\mathbf{x_r}$.

Remark 1. It is important to note that $\mathbf{v_d}$ and $\dot{\mathbf{x}}_\mathbf{r}$ are not always equal. This is because $\mathbf{x_r}$ is not an external reference but depends on the actual helicopter position (closest point on the path criterion). Therefore, if a position error exists ($\tilde{\mathbf{x}}$), then $\mathbf{x_r}$ will move on the path but with a velocity different from the aircraft velocity ($\mathbf{v_d}$) [19]. Consequently, $\mathbf{v_d}$ and $\dot{\mathbf{x}}_\mathbf{r}$ will be equal only when $\tilde{\mathbf{x}} = \mathbf{0}$.

3.2. Stability analysis

Theorem 1. *A helicopter modeled with kinematics equations (2), follows a given geometric path $P \in \Re^3$ at a desired velocity $V_d > 0$ satisfying conditions a), b) and c), if the control actions are defined by (3).*

Proof. Control law $\mathbf{v_a}$ (3) can be substituted into the kinematic model (2) to obtain the following closed loop equation

$$\begin{aligned}\dot{\mathbf{x}} &= \mathbf{J}\mathbf{J}^{-1}\mathbf{y} = \mathbf{y}\\ \dot{\mathbf{x}} &= \mathbf{K_s}\tanh(\mathbf{K}\tilde{\mathbf{x}}) + \mathbf{v_d}\\ \mathbf{0} &= (\mathbf{v_d} - \dot{\mathbf{x}}) + \mathbf{K_s}\tanh(\mathbf{K}\tilde{\mathbf{x}})\end{aligned} \tag{6}$$

In general, the desired velocity vector $\mathbf{v_d}$ is different from the time derivative of the desired location $\dot{\mathbf{x}}_\mathbf{r}$, so, defining the velocity difference vector $\boldsymbol{\delta} = \dot{\mathbf{x}}_\mathbf{r} - \mathbf{v_d}$, (6) can be written as

$$\dot{\tilde{\mathbf{x}}} + \mathbf{K_s}\tanh(\mathbf{K}\tilde{\mathbf{x}}) = \boldsymbol{\delta}. \tag{7}$$

Note that the linear velocity components of $\mathbf{v_d}$ and $\dot{\mathbf{x}}_\mathbf{r}$ are collinear (tangent to the path).

Now, to prove the stability of the equilibrium point $\tilde{\mathbf{x}} = [\tilde{x} \;\; \tilde{y} \;\; \tilde{z} \;\; \tilde{\psi}]^{\mathrm{T}} = \mathbf{0}$, it is considered the following Lyapunov Function Candidate

$$V = \frac{1}{2}\tilde{\mathbf{x}}^{\mathrm{T}}\tilde{\mathbf{x}}, \tag{8}$$

and its derivative along the system's trajectories

$$\dot{V} = \tilde{\mathbf{x}}^{\mathrm{T}}\dot{\tilde{\mathbf{x}}} = \tilde{\mathbf{x}}^{\mathrm{T}}\left(-\mathbf{K_s}\tanh(\mathbf{K}\tilde{\mathbf{x}}) + \boldsymbol{\delta}\right). \tag{9}$$

It is obtained the following condition in order to guarantee that $\dot{V}$ be definite negative

$$|\tilde{\mathbf{x}}^{\mathrm{T}}\mathbf{K_S}\tanh(\mathbf{K}\tilde{\mathbf{x}})| > |\tilde{\mathbf{x}}^{\mathrm{T}}\boldsymbol{\delta}|. \tag{10}$$

Next, (10) is investigated in a single dimension (error $\tilde{x}$) to simplify the analysis. A similar study can be done with errors $\tilde{y}$, $\tilde{z}$ and $\tilde{\psi}$.

For large values of $\tilde{x}$, the condition (10) can be reinforced as

$$|k\tilde{x}| > |\delta_x\tilde{x}|, \tag{11}$$

where $k' = k_{sx}\tanh(k_x\tilde{x}_{aux})$ and $\tilde{x}_{aux}$ is the minimum value at which the error can be considered large. Thus, one condition for $\dot{V}$ to be negative definite is

$$k_{sx} > \frac{|\delta_x|}{|\tanh(k_x\tilde{x}_{aux})|}. \tag{12}$$

Condition (12) establishes a design parameter to make error $\tilde{x}$ to decrease.

Now, for small values of $\tilde{x}$ ($\tilde{x} < \tilde{x}_{aux}$) the condition given by (10) would be satisfied if

$$\left|\frac{k'}{\tilde{x}_{aux}}\tilde{x}^2\right| > |\delta_x\tilde{x}|; \tag{13}$$

which means that a sufficient condition for $\dot{V}$ to be negative definite is

$$|\tilde{x}| > \frac{|\delta_x||\tilde{x}_{aux}|}{|k_{sx}\tanh(k_x\tilde{x}_{aux})|}, \tag{14}$$

thus implying that error $\tilde{x}$ is ultimately bounded by

$$|\tilde{x}| \leq \frac{|\delta_x||\tilde{x}_{aux}|}{|k_{sx}\tanh(k_x\tilde{x}_{aux})|}. \tag{15}$$

Once the control errors are inside the bound (to errors $\tilde{y}$, $\tilde{z}$ and $\tilde{\psi}$ the bounds are similar to (15)), that is with small values of $\tilde{\mathbf{x}}$, $\mathbf{K_s}\tanh(\mathbf{K}\tilde{\mathbf{x}}) \approx \mathbf{K_s}\mathbf{K}\tilde{\mathbf{x}}$. Now it is proved by contradiction that these control errors tend to zero.

The closed loop equation (7) can be written after the transient as

$$\dot{\tilde{\mathbf{x}}} + \mathbf{K_s}\mathbf{K}\tilde{\mathbf{x}} = \boldsymbol{\delta}, \tag{16}$$

or in Laplace transform form

$$\tilde{\mathbf{x}}(s) = (s\mathbf{I} + \mathbf{K_s}\mathbf{K})^{-1}\boldsymbol{\delta}(s). \tag{17}$$

According to (17) and recalling that $\mathbf{K_s}$ and $\mathbf{K}$ are positive constant diagonal matrices, the control error vector $\tilde{\mathbf{x}}$ and velocity difference vector $\boldsymbol{\delta}$ cannot be orthogonal. Nevertheless, both vectors are orthogonal by definition (see *Remark 1* and remember the minimum distance criteria for $\mathbf{x_r}$ on P). Therefore, the only solution for steady state is that $\tilde{\mathbf{x}}(t) \to \mathbf{0}$ asymptotically (condition a) and c)), and consequently, $V_a(t) \to V_d(t)$ (condition b)).

4. Determining the Path Speed

In this proposal, the desired speed of the helicopter is a function of the assigned path. As mentioned

above, one desires to accomplish the mission as quickly as possible in order to save energy. But, as a consequence, it can lead to unacceptable position errors. Then, one way of penalizing the velocity value is considering the path curvature, which gives a quantitative idea of the geometrical requirements.

4.1. Path Curvature

Intuitively, the curvature is the amount by which a geometric object deviates from being flat, or straight in the case of a line. For a given set of points that form a required path r, the curvature value is given by

$$\Gamma(t) = \frac{\left\| \frac{dr}{dt} \times \frac{d^2 r}{dt} \right\|}{\left\| \frac{dr}{dt} \right\|^3}. \tag{18}$$

Once the curvature of the path could be found at each point, the desired speed v_d for kinematic controller is proposed as

$$V_d = f(V_{\max}, \Gamma) \Rightarrow V_d = \frac{V_{\max}}{1 + k_{sc} \tanh[k_c |\Gamma(i+N)|]}, \tag{19}$$

where $k_c > 0$ is a tuning parameter that sets the minimum value of V_d, and $V_{\max}$ is the maximum speed at which the aircraft can navigate (in terms of their physical limitations and the application). Because the path is known, it is possible to use the value of curvature at N points forward (prediction), to attenuate the desired speed with anticipation and allow the reaction of the low-level control at time. Thus the proposed speed is bounded between

$$\frac{V_{\max}}{1 + k_{sc}} \leq V_d \leq V_{\max}.$$

$$\begin{cases} v_{ax} = k_{sx} \tanh\left(k_x \left(x_r - x_a\right)\right)\cos\left(\psi_a\right) + k_{sy} \tanh\left(k_y \left(y_r - y_a\right)\right)\sin\left(\psi_a\right) + V_d \cos\left(\alpha_r\right)\cos\left(\psi_r - \psi_a\right) \\ v_{ay} = -k_{sx} \tanh\left(k_x \left(x_r - x_a\right)\right)\sin\left(\psi_a\right) + k_{sy} \tanh\left(k_y \left(y_r - y_a\right)\right)\cos\left(\psi_a\right) + V_d \cos\left(\alpha_r\right)\sin\left(\psi_r - \psi_a\right) \\ v_{az} = k_{sz} \tanh\left(k_z \left(z_r - z_a\right)\right) + V_d \sin\left(\alpha_r\right) \\ \omega_{az} = k_{s\psi} \tanh(k_\psi \left(\psi_r - \psi_a\right)) \end{cases} \tag{20}$$

■

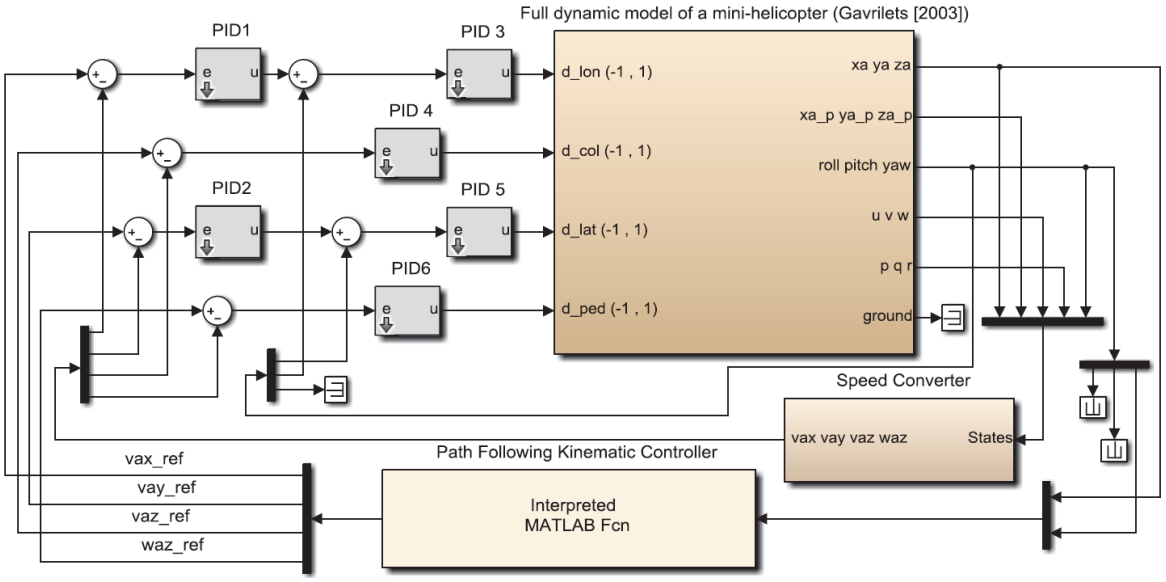

Figure 2. Kinematic path following controller coupled to dynamic model of a mini-helicopter

5. UAV Dynamic Model Coupled to the Kinematic Controller

The dynamic model of UAV presented in [18] and here used to couple the kinematic controller is a very realistic nonlinear model of a mini-helicopter. The model considers helicopter dynamics such as shake, drags and actuator dynamics. Moreover it describes the states of hover and translational flight at low speed accurately. Nominal vehicle parameters are used in our simulations and they correspond to the X-Cell 60 helicopter from Massachusetts Institute of Technology.

The kinematic controller proposed in Section 3 is coupled in such dynamic model in order to evaluate

the proposed controller in a more realistic scenario. Fig. 2 shows the block diagram in Matlab/Simulink used in the simulation and how this coupled is done.

The block *Path Following Kinematic Controller* contains the path following algorithm described in Section 3 and its inputs are the position values (x_a, y_a, z_a) and heading ψ_a of the aircraft, which are output parameters of the dynamic model. The outputs of the kinematic controller are the necessary speed values v_{ax}, v_{ay}, v_{az} and ω_{az} for the vehicle to follow the desired path at the desired speed according to (3) and (4) (xpressed in extended form in (20)). These calculated values become speed references for the entry of the dynamic model (hence the nomenclature $v_{ax_{ref}}, v_{ay_{ref}}, v_{az_{ref}}$ and $\omega_{az_{ref}}$ in Fig. 2).

Six PID controllers are used (analogous to that used in [20]) in order the helicopter to follow the speed references calculated by the kinematic controller. Thus, PID1 controller generates the reference angle (pitch) that is necessary for the helicopter to move with a speed $v_{ax_{ref}}$ and PID2 controller generates the reference angle (roll) that is required to move with a speed $v_{ay_{ref}}$. Then, to achieve these reference angles PID5 and PID3 controllers are used, generating the longitudinal and lateral commands respectively, which are applied to the helicopter servos. Besides, to achieve the speed $\omega_{az_{ref}}$ and $v_{az_{ref}}$, PID4 and PID6 controllers are used respectively, generating the corresponding commands to servos (collective and pedal).

In order to get the signals needed to generate the error signal of these PIDs, it is necessary to take the outputs of the dynamic system and make a speed transformation. This is done in the block *speeds converter* in which the six linear and angular velocities of the helicopter dynamic model (expressed in its coordinate system $\langle s \rangle$) are converted to four speeds v_{ax}, v_{ay}, v_{az} and ω_{az} using a rotation matrix which depends on the angles of pitch and roll [21] given by

$$\begin{bmatrix} v_{ax} \\ v_{ay} \\ v_{az} \\ \omega_{az} \end{bmatrix} = \begin{bmatrix} c_\theta & s_\varphi s_\theta & c_\varphi s_\theta & 0 & 0 & 0 \\ 0 & c_\varphi & -s_\varphi & 0 & 0 & 0 \\ -s_\theta & s_\varphi c_\theta & c_\varphi c_\theta & 0 & 0 & 0 \\ 0 & 0 & 0 & 0 & \frac{s_\varphi}{c_\theta} & \frac{c_\varphi}{c_\theta} \end{bmatrix} \begin{bmatrix} u \\ v \\ w \\ p \\ q \\ r \end{bmatrix}.$$

6. Simulation Results and Discussion

This section presents some simulation results considering the proposed controller. First, it is presented a relationship between the N parameter and the square position error during the mission. In the sequence, some comments considering a fixed value of the N parameter are done for a sinusoidal reference path. Finally, results taking into account other reference paths are also presented. In all the figures, the red (gray) lines are the references and the black lines are the actual values.

Considering an arbitrary curve, the proposed kinematic controller should be adjusted to get information about the curvature of the whole path. It is essential to guarantee the effectively mission accomplishment by the aircraft in cases where the curvature increases, and the maneuver should be more aggressive.

The following simulations consider a sinusoidal path reference with $V_{max} = 5$ m/s, $k_{sc} = 2$ and $k_c = 3$, which means that the minimum speed is $V_{\max}/3$ m/s (for a large curvature), and then $V_{max}/3 \le V_d \le V_{\max}$. The adopted kinematic controller's constants are: $k_x = k_z = 1.6$, $k_y = 1.4$, $k_\psi = 1.8$ and $k_{si} = 1.5$ (where $i = x, y, z, \psi$).

In this first simulation the idea is to highlight the importance of the prediction horizon (defined by the value of N) in the path following error. In other words, the value of N depends on how quickly the PID controller can respond in order to achieve the rotorcraft desired speed. It is worthy to keep in mind that if the system response is slow, it is required a large N value (a longer horizon of curvature prediction), because the desired velocity should be reduced before reaching the curve of interest.

Successive simulations are run for a fixed period of 40 seconds each, for a sinusoidal reference path of 30 m amplitude and 38 m length (period), varying the parameter N between 0 and 100. The mean square position error (MSE) is calculated for each simulation and its relationship with the parameter N can be seen in Fig. 3. Notice that the smallest error is achieved for $N = 52$ (0.092 m) where the traveled path (TP) is 235 m. A longer path can be covered with $N = 0$ (237 m) but the MSE increases, which does not justify the extra traveled path. In the following simulations, $N = 52$ is adopted.

The present work aims to answer the question "which are the advantages of following a path with a variable velocity instead of a fixed one previously tuned for the whole path?" The answer, and some conclusions about the proposed strategy, can be found in the next simulation. It aims to compare the path following mission of a sinusoidal curve during 140 seconds considering a fixed velocity ($V_d = cte$) and a variable one ($V_{\min} < V_d < V_{\max}$). In both cases, MSE and TP are computed to get the idea of 'useful path'.

In order to defined the fixed velocity, the MSE is calculated for a TP considering a set of fixed V_d (staring from 0.2 to 4 m/s, with step of 0.2 m/s). Fig. 4(a)

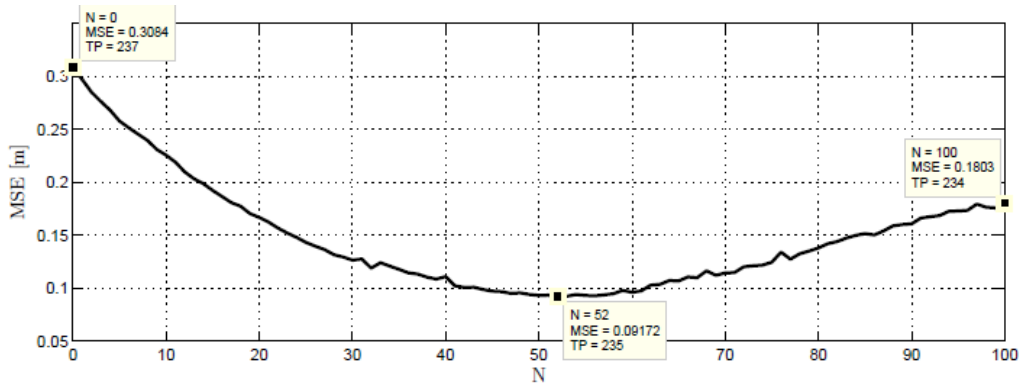

Figure 3. Mean square position error (MSE) for a sinusoidal path, considering different values of the parameter N

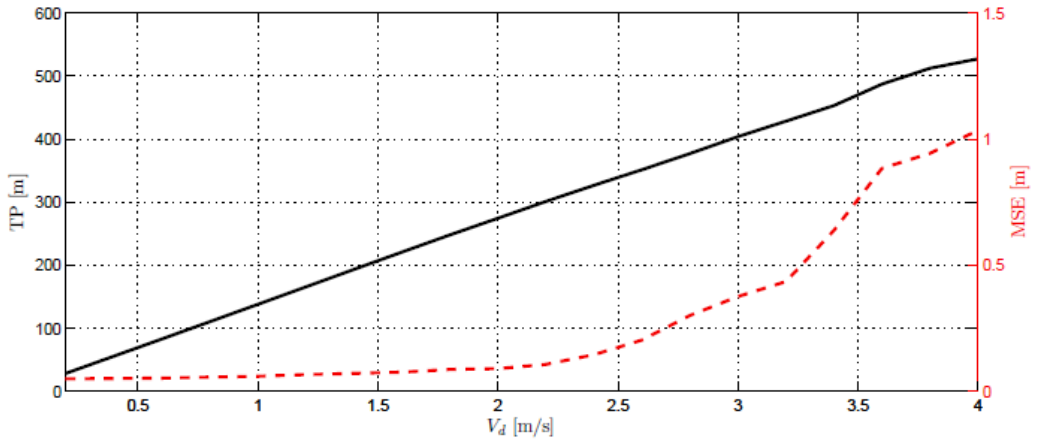

(a)

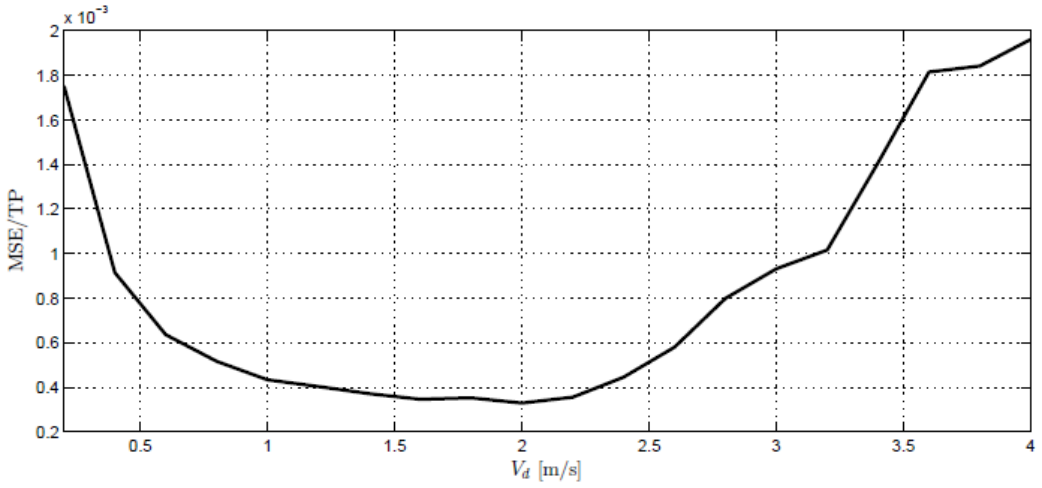

(b)

Figure 4. Relationship of V_d with TP (traveled path) and MSE (mean square position error) (a) and with the ratio MSE/TP (b)

highlights the relationship between the velocity and TP, as well as the velocity and MSE. One can notice that as the velocity increases both MSE and TP rise. The best fixed velocity in the aforementioned set can be obtained by the ratio between the MSE and TP, as show in Fig. 4(b), giving the idea of 'useful path'. The velocity that minimizes such ratio is 2 m/s, which will be adopted to compare with the strategy proposed here.

It is worth mentioning that the helicopter is unable to follow the desired path with velocities above 4 m/s. The maximum fixed speed adopted is 4 m/s, because above this value the aircraft fails to track the reference with tolerable error. this is clearly seen in Fig. 5 for a fixed speed of 4.2 m/s.

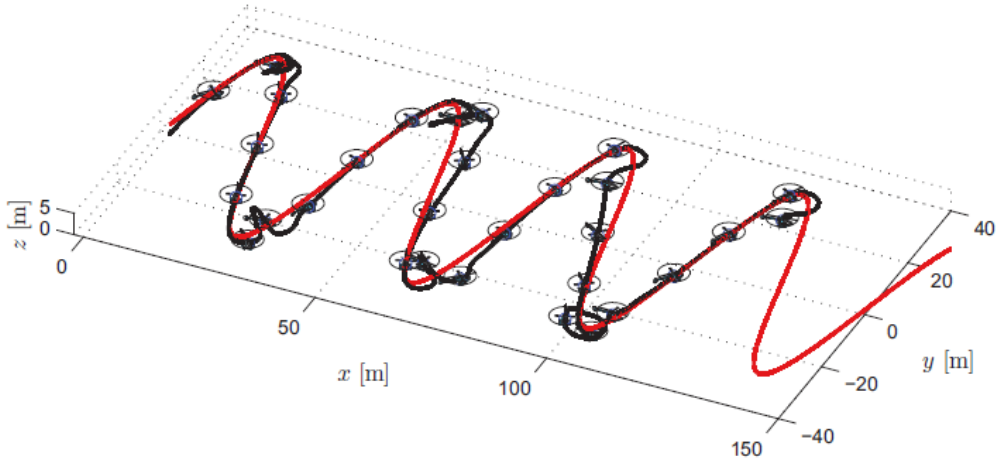

Figure 5. Sinusoidal path at constant velocity $V_d = 4.2$ m/s

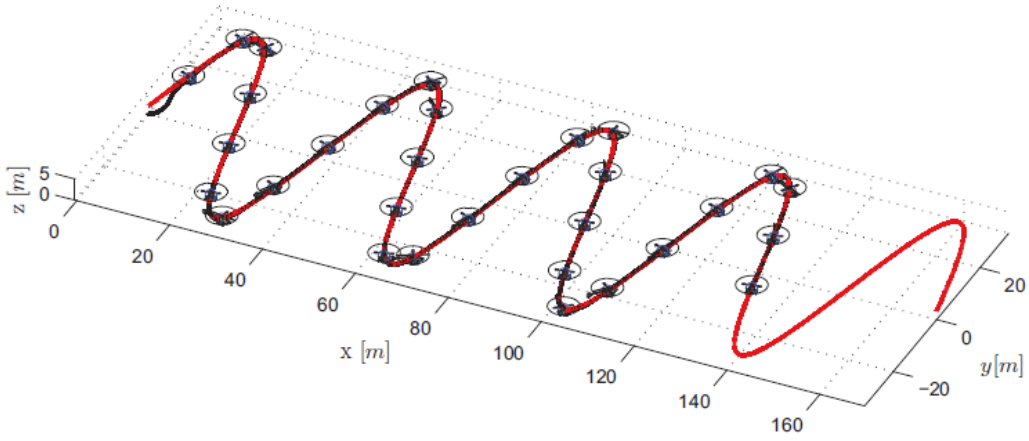

(a)

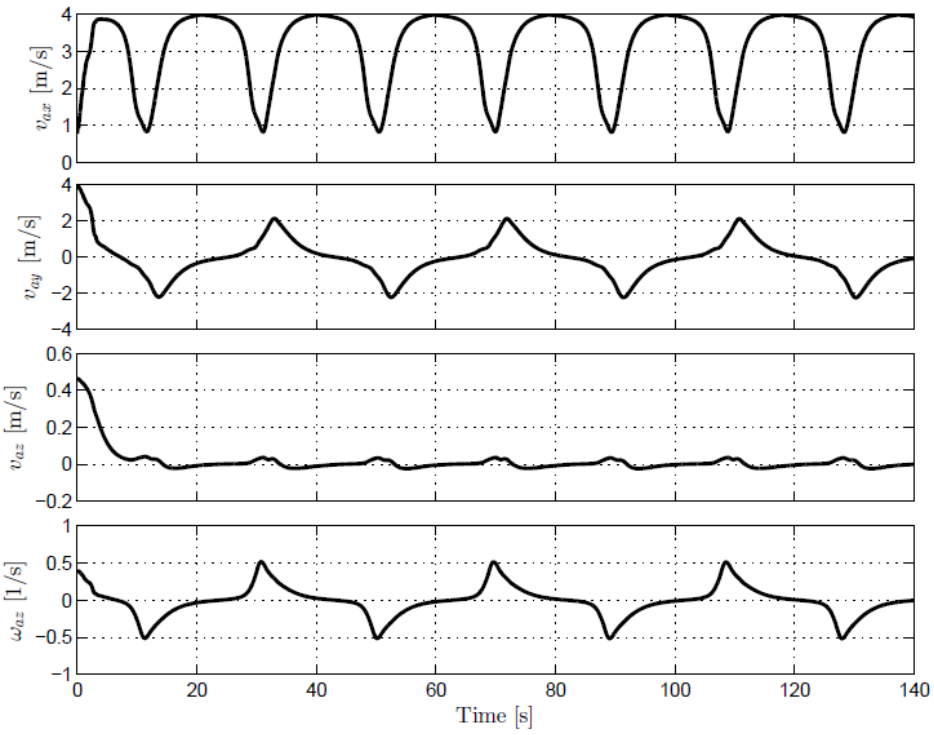

(b)

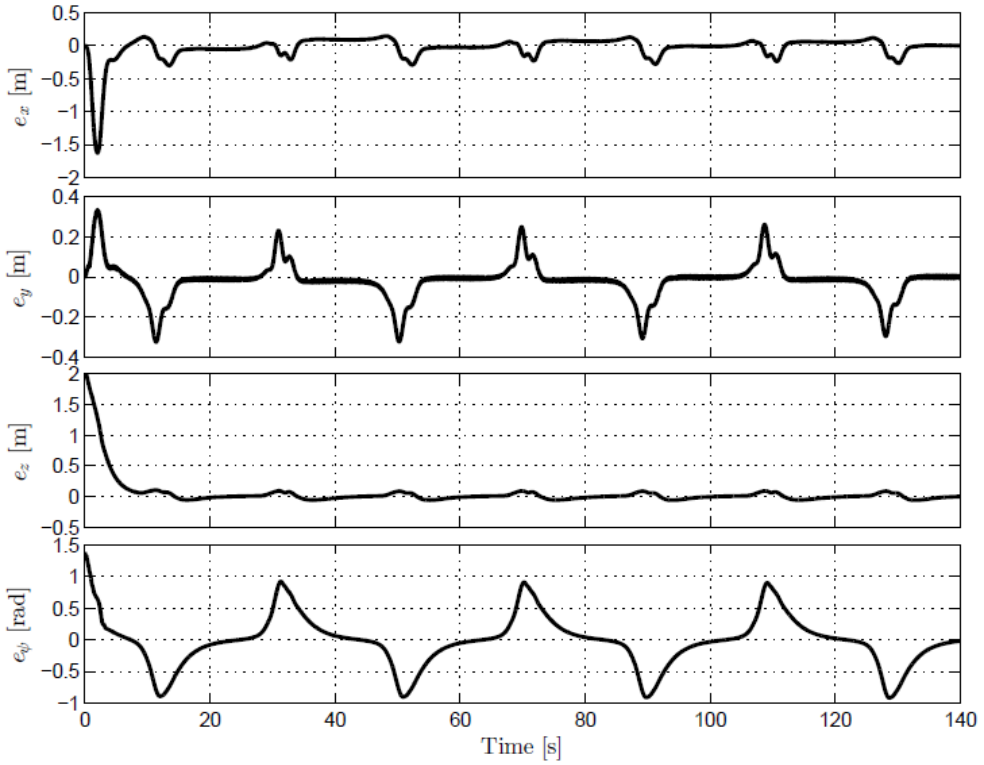

(c)

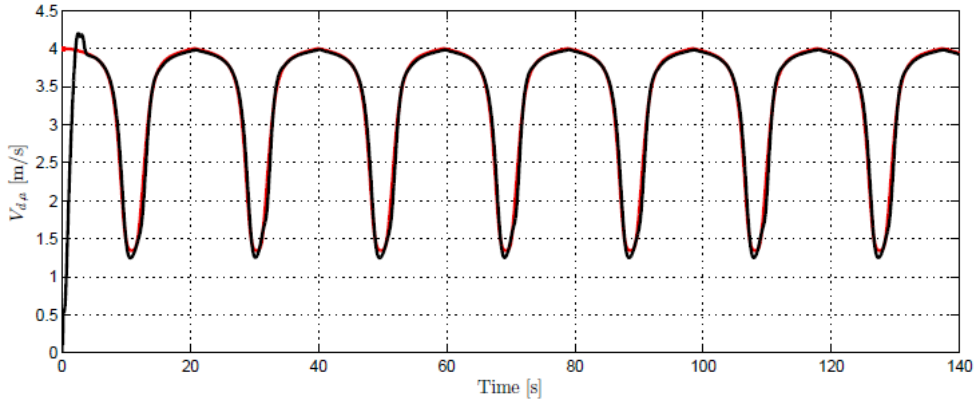

(d)

Figure 6. (a) 3D view of the sinusoidal traveled path, (b) control signals calculated by the kinematic controller, (c) position and orientation errors, and (d) V_d (red) and V_a (black) helicopter velocities when $V_d = f(V_{max}, \Gamma)$

Fig. 6(a) shows the path in the space in the case of variable speed depending on the curvature, where $V_{max} = 4$ m/s is adopted. On the other hand, the desired and actual speeds of the aircraft are shown in Fig. 6(d) and the control actions calculated by kinematic controller in Fig. 6(b). Position and orientation errors for this path are shown in Fig. 6(c), where it is possible to see that the errors increase on path bends and are greatly reduced in the straight parts, tending to zero. In Fig. 6(d), one can notice that the vehicle increases its velocity in the straight portions (tending to V_{max}) and reduces it as the curvature increases.

Considering a fixed and preset velocity, $V_d = 2$ m/s, the traveled path is approximately 275 m, with a position MSE of 0.1 m. Now taking into account the speed as a function of the curvature, the traveled path is 465 m, with a position MSE of 0.15 m. It means that the distance covered is 69% greater in the best scenario of preset velocity. Moreover, for an error around 0.15 m, the helicopter needs to travel with a constant velocity V_d equal to 2.4 m/s (see Fig. 4(a)). In such case, the traveled path is 326 m. Therefore, for the same MSE, the vehicle travels 43% more path using the proposed strategy (the speed as function of the curvature).

Observing Fig. 4(a), in order to navigate 465 m during a path following mission, the fixed velocity should be approximately 3.5 m/s. However, in such case, the position MSE is 0.75 m, which is five times greater than in the variable velocity approach.

A spiral path is proposed as another path reference for 140 seconds of simulation time. Fig. 7 shows the spiral path followed by the helicopter at variable speed according to (19) ($V_{max} = 4$ m/s), and also shows the involved speeds. For this case, the covered path is 427 m with a position MSE of 0.0495 m using the variable speed based on the curvature.

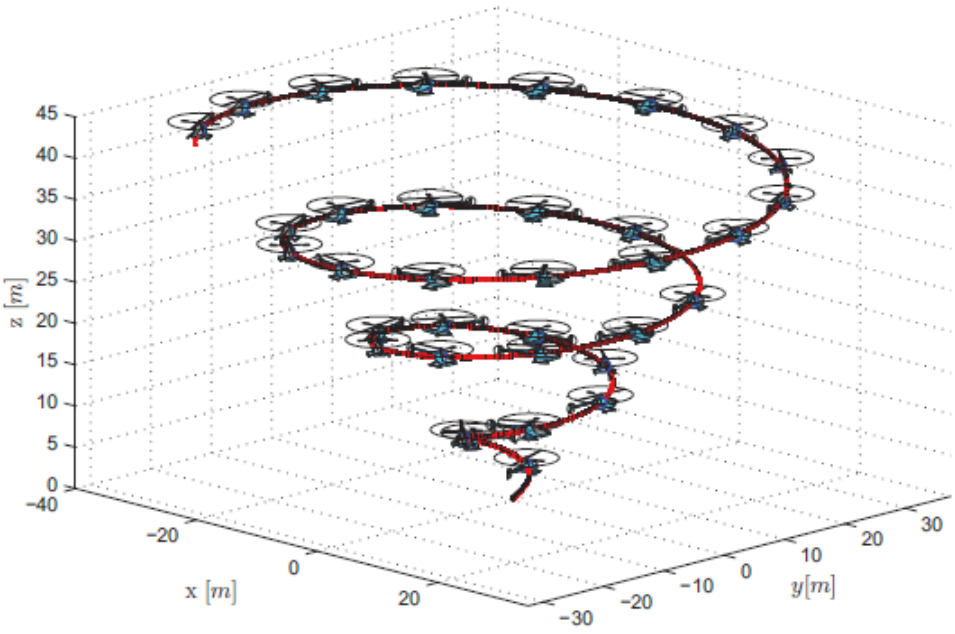

(a)

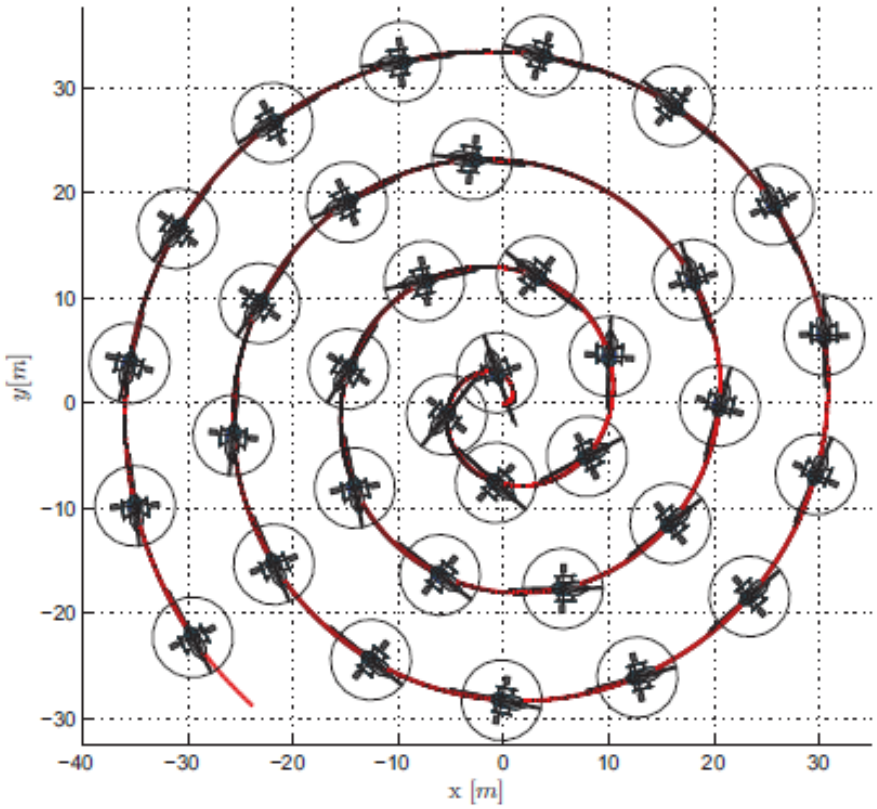

(b)

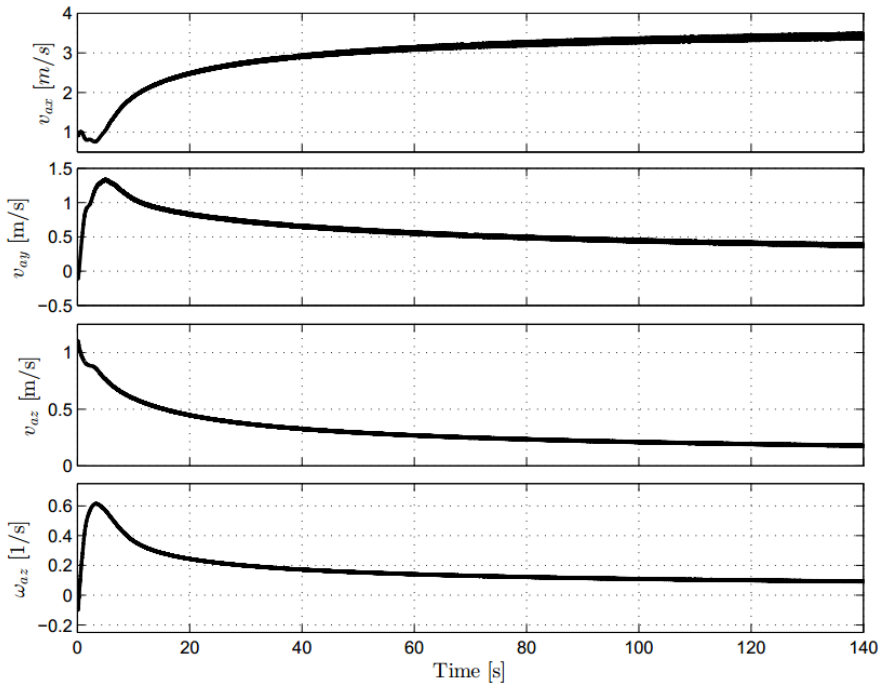

(c)

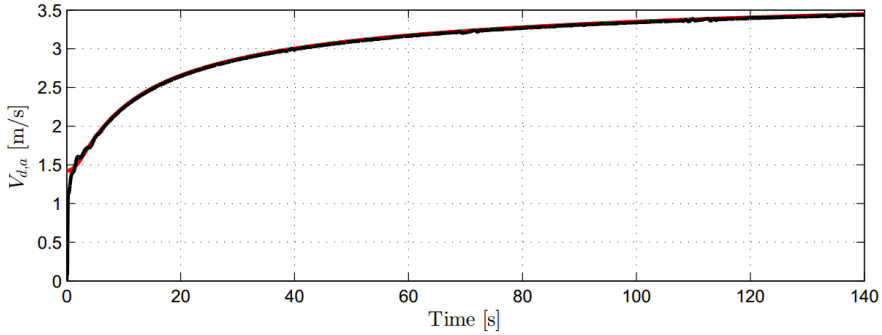

(d)

Figure 7. Spiral path and velocities of the helicopter when $V_d = f(V_{max}, \Gamma)$. (a,b) 3D and XY views of the traveled path, respectively; (c) control signals calculated by the kinematic controller, and (d) V_d and V_a velocities

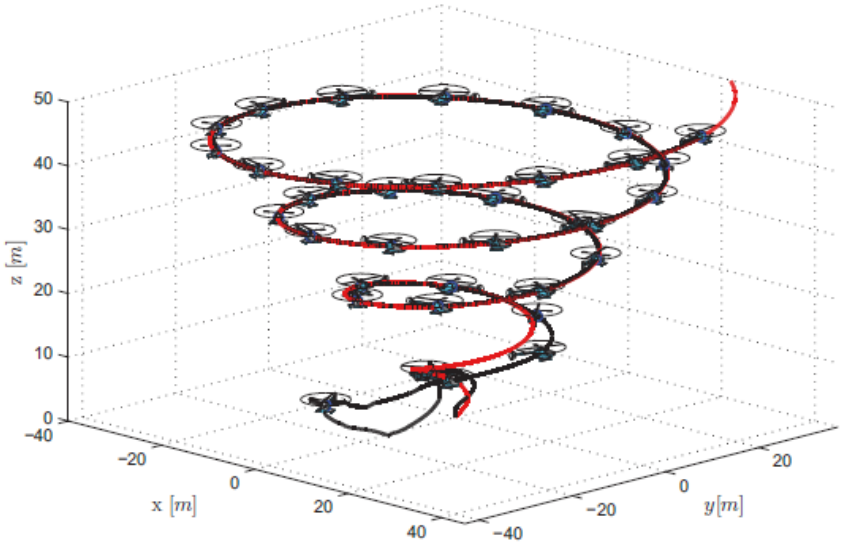

Figure 8. Spiral path at constant velocity $V_d = 4$ m/s

If it follows this same path at fixed speeds from 1 to 4 m/s it is possible to obtain the results shown in Table 1. As can be seen, for similar position error (approximately 0.046 m), the helicopter is capable to cover 427 m in the case of speed as a function of curvature and 278 m at fixed speed. This is a 54% more of covered path for the speed according to (19). Fig. 8 shows how the aircraft fails to follow the path at the beginning (at speed of 4 m/s) where the curvature is more pronounced. This is why the position error is unacceptable.

Table 1. Traveled path (TP) and mean square position error (MSE) for spiral path.

V_d [m/s]	TP [m]	MSE [m]
1	139	0.22
2	278	0.046
3	427	0.12
4	600	1.3

7. Concluding Remarks

Rotary-wing aircraft generally include those heavier-than-air flying machines where one or more rotors are required to provide lift throughout the entire flight, such as helicopters; hence they spend a significant proportion of their available energy maintaining their own weight in the air. Based on this problem and using a degree of freedom offered by the path following control approach, this paper proposed a path following controller employing a simplified kinematic model of a helicopter, which then has been coupled to a dynamic model of a mini-helicopter through an adaptation stage. The speed during the path following mission is a profile defined by the geometric requirements of the path; then the controller guides the helicopter through the reference path as quickly as possible without neglecting control errors. The stability of the control law was demonstrated using Lyapunov theory and simulation results show the good performance of the proposed controller.

This paper also reported comparison results between variable velocity and fixed velocity profiles. The chosen fixed velocity comes from an exhaustive study taking into consideration the most appropriate value of the prediction horizon N and the relationship between the mean square position error and the traveled path.

According to the simulations results presented here, for an equal position error, 43% (139 m) and 54% (149 m) of extra path can be covered in the sinusoidal and spiral path references respectively using the proposed approach of variable speed. These results can been interpreted in a different way, for example: for the spiral reference at fixed speed $V_d = 2$ m/s the helicopter traveled 278 m with a MSE of 0.046 m in 140 s, and with variable speed as a function of curvature the helicopter traveled 427 m in 140 s with the same MSE; this means that with the latter approach, a distance of 278 m could be covered by the helicopter in less time; and less time in the air is less energy involved.

Furthermore, considering that the controller is based on the kinematic model of a rotorcraft, it provides the flexibility to be used in other rotary-wing UAV changing only the adaptation stage. Moreover, according to its configuration, the speed at which the path is traveled can be chosen based on other aspects of interest.

References

[1] **I. Tjernberg, J. Lindberg, K. Hansson.** *Cooperative Networked Control of Unmanned Air Vehicles*. KTH Electrical Engineering, Stockholm, Sweden, Bachelor's Degree Project, 2011.

[2] **J. F. Roberts, J. C. Zufferey, D. FloreaNo.** Energy Management for Indoor Hovering Robots. In: *Proc. of the IEEE/RSJ Int. Conf. on Intell. Robots and Syst.*, Acropolis Convention Center, France, 2008, pp. 22–26.

[3] **A. S. Brandão, D. Gandolfo, M. Sarcinelli-Filho, R. Carelli.** PVTOL Maneuvers Guided by a High-Level Nonlinear Controller Applied to a Rotorcraft Machine. *European J. of Control*, 2014, Vol. 20, No. 4, 172–179.

[4] **H. Boudjedir, O. Bouhali, N. Rizoug.** Neural Network Control Based on Adaptive Observer for Quadrotor Helicopter. *Int. J. of Inf. Tech., Control and Autom.*, 2012, Vol. 2, No. 3, 39–54.

[5] **B. Erginer, E. Altuğ**. Design and Implementation of a Hybrid Fuzzy Logic Controller for a Quadrotor VTOL Vehicle. *Int. J. of Control, Autom. and Systems*, 2012, Vol. 10, No. 1, 61–70.

[6] **M. Abdolhosseini, Y. Zhang, C. A. Rabbath.** An Efficient Model Predictive Control Scheme for an Unmanned Quadrotor Helicopter. *J. of Intelligent & Robotic Systems*, 2013, Vol. 70, No. 1-4, 27–38.

[7] **C. Rosales, D. Gandolfo, G. Scaglia, M. Jordan, R. Carelli.** Trajectory Tracking of a Mini Four-Rotor Helicopter in Dynamic Environments - a Linear Algebra Approach. *Robotica*, 2015, Vol. 33, No. 8, 1628–1652.

[8] **C. Papachristos, K. Alexis, A. Tzes.** Linear Quadratic Optimal Trajectory-Tracking Control of a Longitudinal Thrust Vectoring-Enabled Unmanned Tri-Tiltrotor. In: *Proc. of the IEEE Annual Conf. on Industrial Electronics Society (IECON)*, 2013, pp. 4174–4179.

[9] **A. P. Aguiar, J. P. Hespanha, P. V. Kokotovic.** Path-Following for Nonminimum Phase systems removes performance limitations. *IEEE Trans. Autom. Control*, 2005, Vol. 50, No. 2, 234–239.

[10] **Y. Chen, T. Wang, J. Liang, C. Wang, C. Xue.** A Fuzzy Robust Path Following Controller for a Small Unmanned Air Vehicle. In: *Proc. of the IEEE Conf. on Ind. Electron. and App.*, Singapore, 2012, pp. 1189–1194.

[11] **J. Zhang, Q. Li, N. Cheng, B. Liang.** 2-D path Following Control for Unmanned Aerial Vehicles. In: *Proc. of the IEEE Int. Conf. on Computer Science and Autom. Eng.*, Vol. 1, May 2012, pp. 585–589.

[12] **L. R. G. Carrillo, A. Dzul, R. Lozano.** Hovering Quad-Rotor Control: A Comparison of Nonlinear Controllers Using Visual Feedback. *IEEE Trans. Aerosp. Electron. Syst.*, 2012, Vol. 48, No. 4, 3159–3170.

[13] **P. Sujit, S. Saripalli, J. Sousa.** An evaluation of UAV path following algorithms. In: *Proc. of the European Control Conference*, IEEE, 2013, pp. 3332–3337.

[14] **I. Rhee, S. Park, C.-K. Ryoo.** A Tight Path Following Algorithm of an UAS Based on PID Control. In: *Proc. of the SICE Annual Conf.*, Taiwan, August 2010, pp. 1270–1273.

[15] **Y. Wang, P. Zhou, Q. Wang, D. Duan.** Reliable Robust Sampled-Data H_∞ Output Tracking Control with Application to Flight Control. *Information Technology and Control*, 2014, Vol. 43, No. 2, 175–182.

[16] **S. Park, J. Deyst, J. P. How.** Performance and Lyapunov Stability of a Nonlinear Path-Following Guidance Method. *AIAA J. on Guidance, Control, and Dynamics*, November-December 2007, Vol. 30, No. 6, 1718–1728.

[17] **D. Nelson, D. Barber, T. McLain, R. Beard.** Vector Field Path Following for Miniature Air Vehicles. *IEEE Trans. Robot.*, June 2007, Vol. 23, No. 3, 519–529.

[18] **V. Gavrilets.** *Autonomous Aerobatic Maneuvering of Miniature Helicopters.* Ph.D. dissertation, Massachusetts Institute of Technology. Dept. of Aeronautics and Astronautics, Cambridge, MA, 2003.

[19] **V. Andaluz, F. Roberti, J. M. Toibero, R. Carelli.** Adaptive Unified Motion Control of Mobile Manipulators. *Control Engineering Practice*, 2012, Vol. 20, No. 12, 1337–1352.

[20] **L. R. Salinas, E. Slawiñski, V. A. Mut.** Kinematic Nonlinear Controller for a Miniature Helicopter via Lyapunov Techniques. *Asian J. of Control*, 2014, Vol. 16, No. 3, 856–870.

[21] **M. Cook.** *Flight Dynamics Principles: A Linear Systems Approach to Aircraft Stability and Control*. MA: Butterworth-Heinemann, 2012.

Received June 2015.